Development of Multi-Objective Core Optimization Framework and Application to Sodium-cooled Fast Test Reactors

Kaiyue Zeng [1,2], Nicolas E. Stauff [2], Jason Hou [1], Taek K. Kim [2]

[1] *Department of Nuclear Engineering, North Carolina State University, Raleigh, NC 27695, U.S.A.*

[2] *Nuclear Science and Engineering Division, Argonne National Laboratory, Lemont, IL 60439, U.S.A.*

Corresponding author: Kaiyue Zeng [1,2]

[1] *Department of Nuclear Engineering, North Carolina State University, Raleigh, NC 27695, U.S.A.*

[2] *Nuclear Science and Engineering Division, Argonne National Laboratory, Lemont, IL 60439, U.S.A.*

Email: kzeng2@ncsu.edu

Number of pages: 49

Number of tables: 9

Number of figures: 13

Development of Multi-Objective Core Optimization Framework and Application to Sodium-cooled Fast Test Reactors

The optimization of a Sodium-cooled Fast Reactor (SFR) core is a challenging process, due to the large number of design parameters, the nonlinearities among inputs and outputs, and the complicated correlation among output parameters. This study attempts to develop a generalized framework for the SFR core optimization by coupling the sensitivity analysis, advanced optimization algorithm, and optionally the surrogate modeling. The framework is built based on the fast reactor modeling capability of the Argonne Reactor Computation (ARC) suite and the sensitivity analysis and optimization modules embedded in the DAKOTA code, both have been integrated within the NEAMS Workbench. The genetic algorithm is selected as the optimization method for its robustness, while the option of surrogate modeling is also explored to alleviate the computational burden caused by employing the ARC direct core physics simulation and thus enhance the efficiency of the optimization. Finally, the normalized deviations of performance parameters of the near-optimal solution from those of the ideal core are calculated and used as criteria to down select the final core design. The developed framework is applied to the Advanced Burner Test Reactor (ABTR) core, and optimal solutions are determined by balancing various objectives simultaneously, including peak fast flux, core volume, power, reactivity swing, plutonium mass feed, while at the same time satisfying the predefined constraints due to safety or economics considerations. The optimal ABTR core design obtained using the direct physical simulation and surrogated model are compared and discussed. It is found that using the accurately constructed surrogate models can significantly reduce the required computational time while maintaining satisfactory accuracy.

Keywords: Multi-objective optimization; genetic algorithm; sensitivity analysis, SFR, test reactor

1. Introduction

The design of a nuclear reactor commonly consists of an iterative procedure involving the modeling of neutronics, thermal-hydraulics, and fuel mechanics. A number of constraints must be applied during the core design to satisfy the safety requirements through steady state, transient and accident conditions. Finally, the optimal core design must reflect a balance between economic characteristics and safety performance of the core. All of these multi-physics and multi-scale design processes make the core optimization study a complex problem, and performing the core optimization in an efficient and effective manner is thus extremely important.

The classical approach for optimization of the nuclear reactor design is usually performed in different designing steps, each corresponding to one of the physics. These methods commonly rely on the expertise and in-depth knowledge of the problem, and by default assuming variables among different physics to be independent from each other from the optimization point of view. Moreover, analysts generally conduct iterations based on local derivatives of output with respect to input design parameters, making the problem more easily convergent to local optimum instead of global optimum. For example, an optimization method was developed to solve the CANDU reactor design at equilibrium refueling. The first-order generalized perturbation theory and nonlinear programming technique were implemented to search for the optimal solution from a neutronics point of view [1]. The effectiveness of this type of method is limited partially due to the complex correlations among the input design parameters, the strong coupling of the output core performance, and the nonlinearities among inputs and outputs.

One possible alternative method to the classical approach is the use of global optimization method such as the genetic algorithms. Inspired by Darwin's theory of evolution of species [2], the genetic algorithm was proposed by Holland in 1975 [3], and it works by iterating groups of solutions: creating an initial population of solutions, evaluating them and determining the survival solutions, then evolving from parental generation to offspring generation through clone, cross-over, and mutation operations. This process generally mimics the natural selection and the species evolution and does not require any calculation of derivatives. With this feature, the genetic algorithm is applicable to many engineering problems, and has been successfully implemented in nuclear engineering problems for quite a long time.

Genetic algorithms have been used in a wide range of light water reactor design problems, including but not limited to the core design [4], plant design [5], and fuel management [6]. A systematic investigation was performed using genetic algorithms to optimize the reactor core loading pattern and placement of burnable poison assemblies [7, 8, 9], separately [7] or simultaneously [8]. Since optimizations using genetic algorithms require a large number of sample calculations, heuristic rules were used to reduce possible computational time. It was proven that the Haling Power Depletion (HPD) and a linearization technique could be successfully used to reduce computational time and create efficient initial populations. The optimization code was further coupled with the CASMO-4/SIMULATE3 code package for an accurate lattice and core physics optimization and further verified the effectiveness and advantages in saving computational resources of using the HFD technique [9].

In recent years, several attempts were made to extend the use of genetic algorithms in fast reactor optimization problems. The TRIAD method was developed to optimize a SFR core design [10]. Extreme solutions were presented with associated core configurations to enhance the understanding of the global trends for the core performances. The FARM method was developed for fast reactor core predesign optimization and presented in [11, 12], where a set of core output responses and safety estimators were proposed as optimization objectives. Optimization was performed to search a multi-physics design space formulated through neutronics, fuel mechanics, subassembly analysis and thermal-hydraulics. Optimal core designs balancing economics performance and intrinsic safety characteristics during steady state, and protected and unprotected transients were selected and compared. It needs to be highlighted that several analytical models were developed to reduce the complexity of the problem and thus enabled the authors to explore a large number of samples to obtain the optimal core designs. More research [13] made use of the regression or interpolation techniques to mathematically build surrogate models to replace the time consuming direct physical simulations and performed multi-physics core optimization. A methodology for optimizing the highly heterogeneous SFR core predesign was developed, and the artificial neural network was used to construct a surrogate model to replace the deterministic neutron core calculation. Multi-objective optimization was performed with a large sample size to capture the global trade-off of core performances [14].

This paper performs core optimization study based on the NEAMS Workbench platform, which was initiated in 2016 within the US Department of Energy's Nuclear Energy Advanced Modelling and Simulation (NEAMS) [15, 16, 17] to integrate a wide

range of computational tools and provide a universal user interface to facilitate model creation, real-time simulation, execution, output processing and visualization. The Argonne Reactor Computation (ARC) suite of codes has been developed at Argonne National Laboratory since the 1980s for fast reactor analysis and integrated into the NEAMS Workbench [18]. The DAKOTA software [19], an integral toolkit for sensitivity analysis, uncertainty quantification and optimization developed and maintained by Sandia National Laboratory, was also integrated into the NEAMS Workbench [20]. The Workbench allows for these integrated codes to communicate and interact together. DAKOTA has been used to drive the ARC codes to solve sensitivity analysis and uncertainty quantification problem [21], and is used to drive the optimization procedure of the sodium-cooled fast reactor core design in this paper. More specifically, the genetic algorithm optimization modules embedded in DAKOTA software are used in this study, and multi-objective optimization with both direct physics simulation and surrogate models are investigated. The ARC code is used for core modeling, and a surrogate model is built based on the obtained simulation results. Compared to previous works related to SFR core optimization [11, 12, 13, 14], the work performed in this study has the characteristics as summarized below:

- A global sensitivity analysis is performed to obtain the sensitivity coefficient of design objectives with respect to the design parameters and to reveal the correlations between core output responses. The results are utilized to reduce the input space and shorten the list of design objectives. Both will reduce the number of generations required before reaching optimal solutions during the optimization.
- Optimization based on direct physics simulation (i.e., core calculation with ARC) is performed. Surrogate models are built and verified with simulation results obtained

from ARC calculation. Comparison of these two methodologies is discussed in this paper.

- DAKOTA works as a "black-box" tool in driving the optimization procedure, which means that DAKOTA has little awareness of the external code. As a result, it will be easy to extend the framework developed in this paper to other optimization problems, either still relying on ARC for deterministic neutronics calculation or replacing ARC with other core simulators, with very limited modification in DAKOTA input file.

This work is intended to develop a generalized optimization framework for the SFR core design, with the features outlined above, and to perform a case study of its application on the Advanced Burner Test Reactor (ABTR) [22] optimization problem. Section 2 presents the reference ABTR design and performance, obtained using the direct physics calculation method. Section 3 introduces the major constituents of the proposed optimization framework, including the problem setup by specifying the design variables, objectives, and constraints, its refinement using the sensitivity analysis results, the genetic algorithm, and finally the implementation based on the NEAMS Workbench. The multi-objective optimization results for the ABTR core are provided and analyzed in Section 4, which show promising solutions while raising questions about the optimization efficiency. In Section 5, supplemental studies are preformed aiming to alleviate the computational burden by generating fast-running and accurate surrogate models and maintaining a small number of objectives. A comprehensive comparison of the various optimization approaches developed in this study is also conducted to provide a general guidance for the future

application of this framework. Finally, the conclusions of this study are summarized and future work is suggested, as presented in Section 6.

2. ABTR Core Reference Design

The paper focused on developing a generalized framework for SFR core optimization problem. It is applied on the core design optimization of the ABTR, which is a small SFR concept designed for irradiation testing. The design optimization targets improving irradiation testing performance, safety characteristics and core economics. The reference ABTR core design is briefly described in Section 2.1, while a direct physics simulation using NEAMS Workbench is performed in Section 2.2 and the result analysis is presented in Section 2.3.

2.1 Description of the ABTR

The Advanced Burner Test Reactor (ABTR) has been developed under the Global Nuclear Energy Partnership (GNEP) program for demonstrating the transmutation technologies and to support the development of the Advanced Burner Reactors (ABRs). The detail reference core configuration and geometrical dimensions for the metallic fuel core is obtained from the ABTR pre-conceptual report [22]. The ABTR is a pool-type sodium-cooled fast reactor and its core layout is shown in Fig. 1 [22]. It displays 199 assemblies – 54 driver fuel assemblies, 78 reflector assemblies, 48 shield assemblies, 9 test assemblies for material test and fuel test purposes, and 10 primary and secondary control rods. The reactor core is radially divided into two enrichment zones: inner core region and outer core region composed of 24 and 30 driver fuel assemblies, respectively. Two ternary alloy fuels of U-Pu-10%Zr and U-TRU-10%Zr have been considered in the ABTR design [22]. In this

study, however, the ternary of U-TRU-10%Zr with the TRU reprocessed from light water reactor discharge fuel is used. Axially, fuel assembly consists of lower reflector, fuel pin, gas plenum and upper reflector. The ABTR core generates 250 MW thermal power under reference configuration, with a coolant inlet and bulk outlet temperature of 355 °C and 510 °C, respectively.

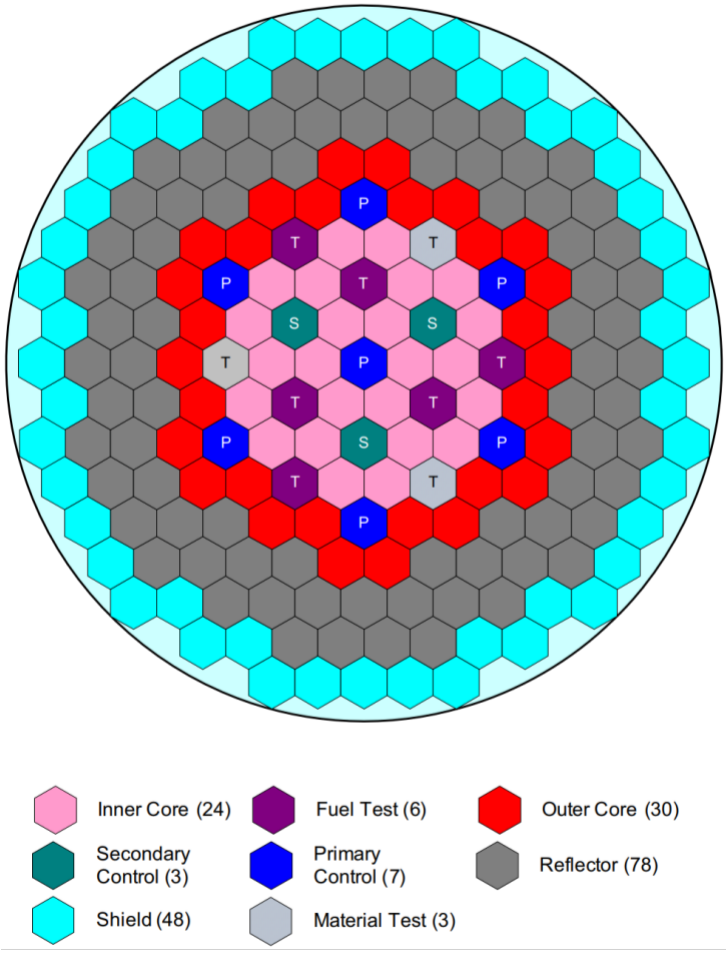

Fig. 1 – Radial cross section of the reference ABTR core [22].

2.2 Direct Physics Core Performance Calculations

The ARC code suite is used to model the ABTR core through the NEAMS Workbench and its PyARC module [15, 18]. The MC$_2$-3 [23] is used to generate reference 33-group cross

sections file that is used for all optimization calculations, and for final evaluation of the optimized solution. The homogeneous multi-group cross-section computation uses a fine 2082 energy group structure based on the ENDF/B-VII.0 nuclear data library [24] and cross sections are condensed into 33 energy groups using buckling search for fuel regions and leakage information from fuel region in the structure regions. The core flux distributions are calculated using the DIF3D code, which has two options to solve the hexagonal-Z nodal diffusion equation (DIF3D/NODAL [25]) and transport equation (DIF3D/VARIANT [26]). Since a large number of flux calculations is expected during the optimization process, the core flux calculation is conducted with the diffusion equation solver, while the transport equation solver is used for reference and final simulations, where flux calculations use 3_{rd} order for the angular flux and 1_{st} order for the scattering approximations. For the flux within a node, on the boundary, and for the source within a node, the polynomial orders are 2, 6, and 1, respectively. Core calculations are done with "all rods out" in a three-dimensional core model where fuel assemblies are radially homogenized. Finally, the sodium void worth is calculated with exact perturbation theory using the PERSENT code [27].

Steady-state thermal-hydraulic calculations are performed with a simple 1D model of every driver fuel assembly based on detailed power information extracted from the neutronic calculation to sort fuel assemblies into three flow channels. The hot channel factors (HCF) approach [28] is employed to estimate the peak cladding temperatures while accounting for various sources of uncertainties and unknowns.

Fuel cycle analysis is performed in this study using the REBUS-3 code [29] for TRU enrichment search at equilibrium cycle, such that the reactor maintains criticality

during the desired cycle length. The cycle length of the reference core is 120 days, and the number of batches for the inner core, outer core and test assemblies are 12, 15 and 12, respectively.

2.3 ABTR Reference Core Performance

As presented in Table I, a reference calculation is performed using DIF3D/VARIANT transport solver to obtain ABTR core performance. The core reactivity swing through the equilibrium cycle is 1415 pcm with a cycle length of 4 months and a core average discharge burnup of 89.7 GWd/T. The reactor core is loaded with 4024.1 kg of heavy metal, and the required external heavy metal and Pu feeds are 962.3 kg/year and 178 kg/year, respectively. The core generates 250 MWth and the average power density is 258.0 W/cm^3. The peak fast flux and peak fast fluence are 2.85×10^{15} n/cm^2-s and 3.56×10^{23} n/cm^2, respectively. The TRU enrichments calculated from the REBUS equilibrium enrichment search are 21.70% and 16.87% for the outer core and inner core regions, respectively. Kinetic parameters and thermal-hydraulics responses are also estimated at the beginning of equilibrium cycle (BOEC). The effective delayed neutron fraction and sodium void worth are 334 pcm and -0.352 $, respectively. The peak pressure drop and temperatures are obtained as the maximum values among three thermal-hydraulics channels under both beginning and end of equilibrium cycles (EOEC).

A brief comparison between the transport and diffusion results is also summarized in Table I. The use of diffusion solver in REBUS equilibrium search calculation, and first order flux calculation in PERSENT calculation reduces the computational time from 86.1 minutes to 13.5 minutes with acceptable computational error. Therefore, the hexagonal-Z diffusion option in the DIF3D is mainly used during the optimization procedure to save

computational resources, while DIF3D/VARIANT transport calculations are performed with the selected optimal core designs for verification purpose.

Table I – Comparison of ABTR reference core results.

Output Quantities of Interests	**Transport Solution**	**Diffusion Solution**	**Rel. Error**
TRU enrichment in outer core	21.10%	21.39%	1.4%
Peak assembly power (MW)	5.08	5.07	-0.2%
Power density of active core (W/cm^3)	258.0	258.0	0.0%*
Reactivity swing (pcm)	1415.0	1362.4	-0.1%
Core fuel inventory (kg)	4024.1	4025.5	0.0%*
External feed of heavy metal (kg/year)	962.3	962.3	0.0%*
Average fuel discharge burnup (GWd/T)	89.70	89.59	-0.1%
Peak fast flux (10^{15} n/cm^2-s)	2.83	2.80	-1.0%
Peak fast fluence ($10^{23} n/cm^2$)	3.57	3.51	-1.7%
Delayed neutron fraction (pcm)	334	333	-0.4%
Sodium void (100% void) ($)	-0.352	-0.350	-0.6%
Peak fuel temperature (^0C)	730.8	730.6	0.0%*
Peak Cladding Temperature with 3-σ HCF (^0C)	641.7	641.6	0.0%*
Peak Pressure Drop (MPa)	0.2431	0.2428	-0.1%

*: 0.0% means the relative error is less than 0.05%.

3. SFR Optimization Framework

3.1 Formulation of Optimization Framework

As displayed in Fig. 2, the generalized optimization framework containing five steps for SFR core optimization is presented in this Section and applied to an example based on the ABTR core design, as presented in Section 3.3 – 3.7.

The first step of optimization is to properly define the problem, which involves selecting optimization objectives and constraints, as well as identifying the important parameters to formulate the exploration input space. A global sensitivity analysis is

suggested as the second step to investigate the correlation among core output variables, which represents the global trade-off among core optimization objectives. The sensitivity coefficient between inputs and outputs, which represents the impact of variation in input on the variation of output, should also be calculated in this step to identify the important core design parameters for the optimization problem. A few iterations are expected between step 1 and step 2 to properly set up the core optimization problem.

The third step considers how to select an appropriate optimization methodology for the specific problem. Existing optimization methodologies are divided into gradient-based and derivative-free methods, while the gradient-based methods make use of the derivatives between inputs and outputs to drive the optimization. SFR core design is generally highly nonlinear problems, and one has to use the derivative-free optimization methodologies. Optimization methods can be further divided into global and local methods, which aim to optimize core designs by exploring the global input space or just the vicinities of current data points. Although an exploration of the whole input space must be applied to obtain global optima, the value of the local optimization method should not be neglected as its advantage in accelerating convergence when combined with the global optimization method. Depending on the problem setup, the optimization problem can be divided into two categories: single-objective and multi-objective optimizations. Moreover, multiple objectives can be scaled and transformed into a single objective, which is helpful in accelerating the convergence speed.

The fourth step focuses on improved optimization efficiency. There are multiple methods for refining and accelerating the convergence performance of the optimization calculation. Multivariate regression techniques including Gaussian Process (GP), Artificial

Neural Network (ANN) and polynomial interpolation, can be used to build a surrogate model to reduce computational time as an addition to core direct physical simulation. Moreover, reducing the number of input parameters or output objectives, as well as imposing more restrictions on optimization constraints can also significantly accelerate the convergence.

The optimization calculation is performed by adjusting multiple core design parameters to search for the best solutions. The last step of the framework focuses on finalizing and interpreting the optimization results. In single-objective optimization problems, the best performing solution achieved meeting constraints is directly returned. For multi-objective optimization problems, the best solutions are provided in a so-called Pareto Frontier, which is a clustering of optimal solutions. The selection of final candidate core designs from the Pareto Frontier is a decision-making process, whose criteria are highly dependent on the trade-off considerations for the particular design. Finally, the optimal core designs need to be recalculated using higher-fidelity simulations. At this step, special attention must be given if large error or bias are identified.

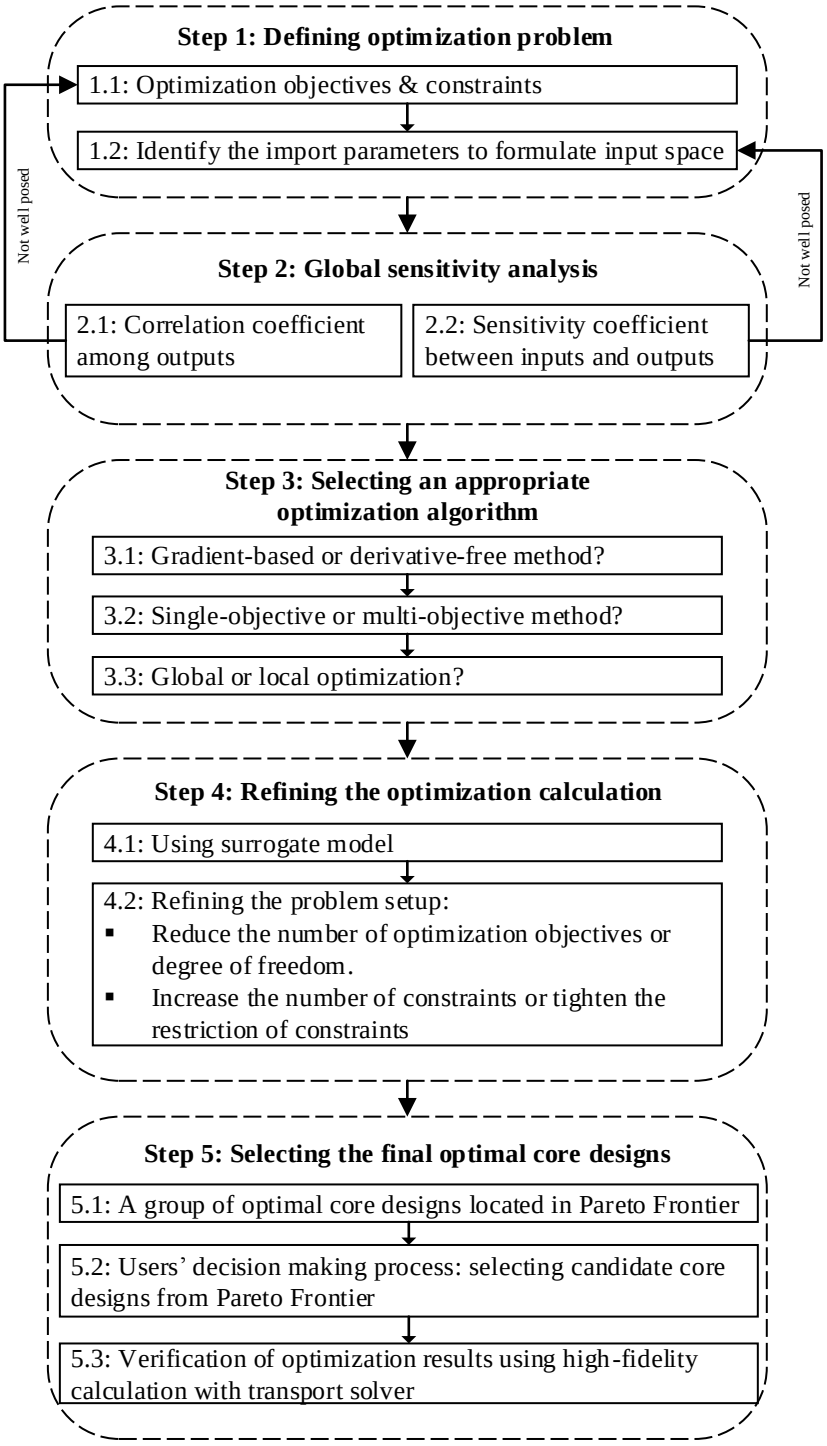

Fig. 2 – Generalized optimization framework applied to SFR core optimization

3.2 Dakota/PyARC coupling within the NEAMS Workbench

The ABTR core optimization is performed using NEAMS Workbench and consisted of the following steps as illustrated in Fig. 3: the ABTR core model is developed using NEAMS Workbench with reference configuration as obtained in [22], and a brief comparison of the simulation results has been presented in Section 2.3. The reference model is further parameterized as a template, with several key design variables picked out as input parameters with predefined exploration bounds. DAKOTA samples each input parameter with the Latin Hypercube Sampling (LHS) technique and generates a user-defined number of ARC inputs, which formulates the initial population. The Workbench driver interface invokes the ARC codes to execute each of the generated inputs, and extracts output responses of interest. Multiple inputs can be executed at the same time at this step. Once the calculations of all inputs are finished, DAKOTA analyzes the extracted output responses, and employs a genetic algorithm to generate the inputs of next generation. This iterative procedure continues until optimization convergence is achieved, with the final generation being the optimal solutions.

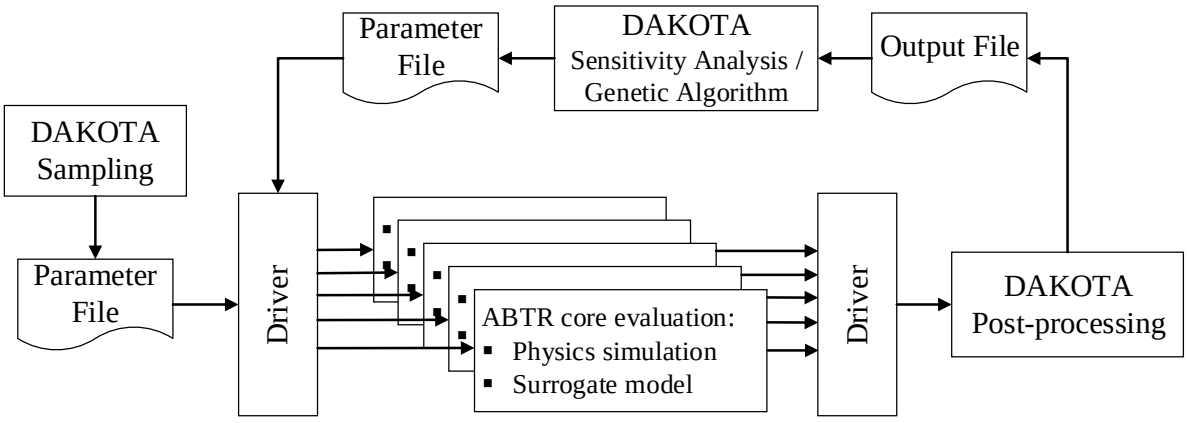

Fig. 3 – The capability of NEAMS Workbench for SFR core sensitivity analysis / optimization.

The Workbench supports flexible communications between DAKOTA and physics simulator through external text files. Upon completion of the simulation, either using direct physics core simulator ARC or evaluating the surrogate model using DAKOTA, a Python post-processing script searches the output file and generates a result file to record important responses of interest readable by DAKOTA. With this feature, this framework is applicable to other types of optimization problems with limited modifications in the Python interface and model development.

3.3 Step 1: Optimization Problem Setup

Properly setting up the case-dependent optimization problem requires effort and expertise. This problem is subdivided into the determination of design goals to be optimized, design constraints to be met, and input parameters to be varied. An example of setting up the ABTR core design optimization is presented in this Section as guidance, while the optimization results are presented in Section 4 and 5 for the purpose of a better explanation.

3.3.1 Optimization objectives and constraints

The reactor core is optimized towards the following objectives under various constraints determined based on core neutronics and thermal-hydraulics performances, safety and economics considerations all along with the reactor's lifetime. In total, five core performance responses are used as optimization objectives, as listed as follows: reactivity swing should be minimized to ensure enough shutdown margin and reduce potential transient over power initiator, core total power and core volume should be minimized to reduce the capital cost of the test reactor; the required yearly external Pu mass feed should be minimized to reduce the fuel cost and requirements; and the peak fast flux needs to be

maximized to provide an optimal irradiation environment for test purpose.

Threshold values of 500 kg/year, 250 MWth, 9.7 m^3, and 2.0×10^{15} n/cm^2-s are enforced in the yearly external Pu mass feed, total core power, core volume, and peak fast flux, respectively. An upper threshold is also placed on reactivity swing to keep it below 2500 pcm to reduce potential transient over power initiator and ensure that the core stays within control rod shutdown margins. Note that these optimization objectives are also used as constraints to accelerate the convergence by directly discarding cases of poor performance. Additional constraints are proposed from the aspects of the material properties and core safety concerns (peak fast fluence, peak temperatures, sodium void worth, and pressure drop along fuel pin), and fuel performances and cost (peak discharged burnup, and TRU enrichment of outer core). In summary, the optimization objectives and constraints applied in this study are presented in Table II.

Table II – Objectives and constraints for ABTR optimization.

Optimization Objectives / Constraints	Goal / Threshold
Reactivity swing	Minimized
Pu mass feed	Minimized
Core power	Minimized
Core volume	Minimized
Peak fast flux	Maximized
Reactivity swing	< 2500 pcm
Pu mass feed	< 500 kg/year
Core power	< 250 MWth
Core volume	< 9.7 m^3
Peak fast flux	> 2.0×10^{15} n/cm^2-s
Maximum TRU enrichment	< 30 w.t.%
Peak fast fluence	< 4.0×10^{23} n/cm^2
Peak discharged burnup	< 200 GWd/T
Peak pressure drop along fuel pin	< 0.5 MPa
Peak cladding temperature	< 650 ℃ with 3-σ HCF
Peak fuel temperature	< 850 ℃

Sodium void worth	< 2 $

3.3.2 Input Space

The input space consists of core design parameters to be optimized with their associated exploration ranges, which are determined based on expertise. As summarized in Table III, seven parameters covering the major reactor geometrical dimensions and fuel cycle analysis are considered for ABTR core optimization, while the rest of input parameters (number of assemblies, the thickness of assembly duct and cladding, etc.) are kept the same as in the reference core configuration. Moreover, three assumptions are made in this optimization problem for the purpose of reducing the number of input parameters:

- The heights of sodium bond relocated in the gas plenum region and of gas plenum are assumed to be 25% and 62.5% of the height of driver fuel column. Axial fuel swelling of 4% is also considered.
- The number of batches for the outer core region is assumed to be 1.25 of that for the inner core region.
- The TRU enrichment of the outer core region is determined from REBUS fuel cycle analysis, while the enrichment of the inner core region is assumed to be 80% of that in the outer core region.

It should be noted that to accelerate the convergence of the genetic algorithm, the continuous core design parameters are discretized into sets of data points before optimization calculation, as also presented in Table III. The numbers of discrete data points for each of the input parameters are given in the second column of Table III, which formulates an exploration input space of more than 11 billion core designs. It is therefore

impractical to go through the whole input design space with a brute force method, and an efficient optimization methodology is required to search for global optima.

Table III – Discretized input parameters.

Input Parameters	Mesh Size	Reference [22]	Exploration Range
Height of the driver fuel column	51	80 cm	50 – 100 cm
Radius of inner cladding surface	73	0.3480 cm	0.2784 – 0.4176 cm
Radius of the wire-wrap structure	24	0.0515 cm	0.0500 – 0.0700 cm
Core total power	41	250 MWth	100 – 300 MWth
Cycle length	61	120 days	50 – 300 days
Number of inner core batch	10	12	3 - 12
Number of pin rings inside fuel assembly	5	9	7 - 11

3.4 Step 2: Global Sensitivity Analysis

A global sensitivity analysis is performed in this Section to obtain the correlation among input parameters and output core responses, and thus examine the reasonability of the problem setup. The Latin Hypercube Sampling (LHS) technique implemented in DAKOTA is used to perform the analysis due to its advantage of achieving convergence with fewer number of samples compared with random sampling method [19]. The seven input parameters are sampled independently based on a uniform distribution, with their lower and upper bounds specified in Table III, to formulate samples of core designs. It is important to first check the convergence of sampling statistics before calculating the global sensitivity coefficients. As displayed in Fig. 4, the mean values and associated standard deviations of reactivity swing are calculated from populations of different sample sizes. It is observed that both the sample size evolving average value and its standard deviation reached convergence after 1500 samples, and the use of a relatively large sample size of 3000 is enough to stabilize the sampling statistics.

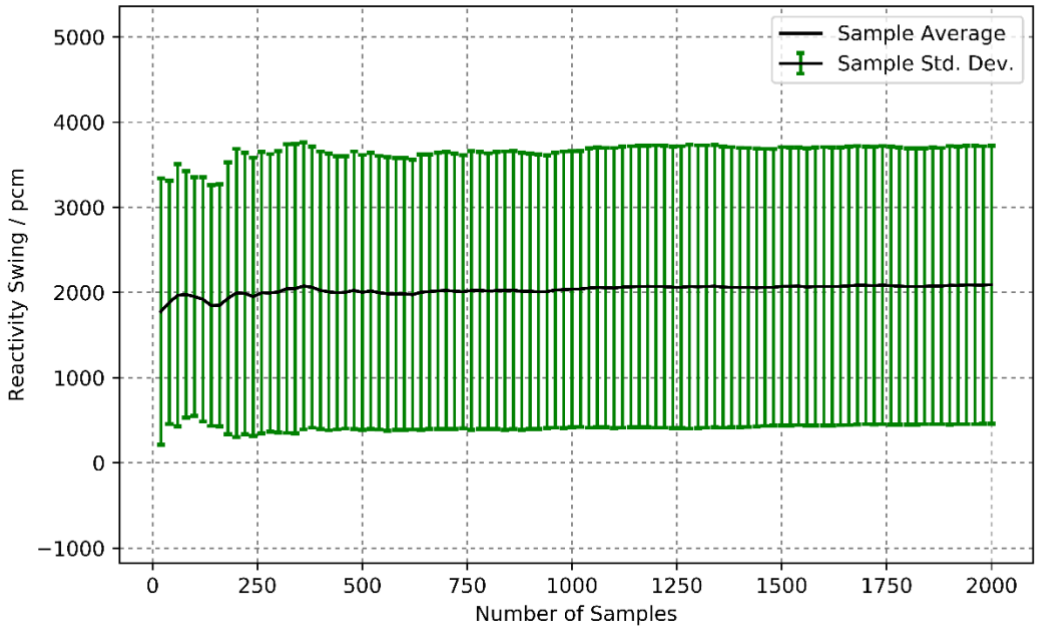

Fig. 4 – Sampling statistics converged after ~ 1500 samples.

The core performances obtained from ARC simulations with associated input core design parameters are extracted for statistical analysis. As shown in Table IV, the Pearson correlation coefficients, which are mathematically computed by dividing the covariance of two variables by the product of their standard deviations and ranged from -1 to +1, are calculated as an evaluation of the linear correlation between input and output variables, as well as between two output variables. A large absolute value of correlation coefficient means that two variables have strong linear associations, where +1 is total positive linear correlation and -1 is total negative correlation. I.e., a negative coefficient indicates that increasing the input results in decreasing output, while a positive coefficient means the input and output tends to change monotonically.

Wire-wrap radius only has significant impacts on peak pressure drop and sodium void worth. In general, the core thermal-hydraulics performances, i.e., peak temperatures and peak pressure drop along fuel pin, are strongly correlated with geometry-related parameters and total power. The correlation is observed to be zero between core power and input parameters, which is due to the fact that the core power is also adopted as an independent input parameter.

The correlations among output responses are also evaluated. The core power is positively correlated with the peak fast flux because decreasing core power tends to reduce the neutron density over the whole core, which also implies that maximizing the core peak fast flux is generally in contradiction of minimizing the core power. The correlation between core power and Pu mass feed is as weak as 0.03, which indicates that there are no obvious linear relations between these two variables. Reactivity swing has a strong positive correlation with peak fast flux. Therefore, a relatively large reactivity swing is expected in the final solutions due to the maximization of peak fast flux. The core power and core volumes are de-correlated parameters since the volume is uniquely determined by core geometrical dimensions, which are adopted as independent input parameters.

Table IV – Correlations among input design parameters and output responses of ABTR core.

		Input Parameters							Objectives				
		Driver Fuel height	Inner Clad Radius	Wire Wrap Radius	Core Power	Cycle Length	Inner Core Batches	Number of Fuel Pin Rings	Δρ	Pu Mass Feed	Core Power	Core Volume	Peak Fast Flux
Objectives	Δρ	-0.28	-0.33	-0.01	0.38	0.55	0.02	-0.48	1				
	Pu Mass Feed	0.12	0.13	0.03	0.03	-0.58	-0.53	0.28	-0.45	1			
	Core Power	-0.01	0.00	0.00	1	0.01	0.00	-0.01	0.38	0.03	1		
	Volume	0.30	0.45	0.08	0.00	-0.01	-0.01	0.82	-0.59	0.33	0.00	1	
	Peak Fast Flux	-0.26	-0.30	-0.05	0.68	-0.04	-0.02	-0.58	0.70	-0.16	0.68	-0.66	1
Constraints	Peak Fast Fluence	-0.13	-0.17	-0.03	0.39	0.55	0.51	-0.32	0.79	-0.59	0.39	-0.37	0.50
	Peak Burnup	-0.23	-0.25	0.01	0.33	0.46	0.41	-0.35	0.84	-0.50	0.33	-0.44	0.54
	Maximum TRU Enrichment	-0.40	-0.48	0.04	0.19	0.25	0.20	-0.55	0.86	-0.41	0.19	-0.74	0.70
	Peak Pressure Drop	0.09	-0.28	-0.21	0.52	0.00	0.00	-0.61	0.62	-0.16	0.52	-0.58	0.84
	Peak Clad Temp.	-0.49	-0.05	0.03	0.59	-0.01	-0.02	-0.59	0.69	-0.18	0.59	-0.62	0.92
	Peak Fuel Temp. BOC	-0.37	-0.01	-0.01	0.61	-0.02	-0.03	-0.66	0.66	-0.18	0.61	-0.64	0.93
	Peak Fuel Temp. EOC	-0.37	0.00	-0.01	0.61	-0.04	-0.03	-0.66	0.65	-0.17	0.61	-0.63	0.93
	Sodium Void Worth	0.69	0.47	-0.11	0.04	0.08	0.07	0.51	-0.51	0.22	0.04	0.82	-0.58

3.5 Step 3: Optimization of ABTR Core Design

In this study, the genetic algorithm based multi-objective optimization capability available in DAKOTA is selected to optimize the ABTR core design and the results will be discussed in Section 4.

As illustrated in Fig. 5, the basic idea of genetic algorithm originates from biological processes, and works by firstly creating a group of core designs (chromosomes) as the initial population through random sampling, evaluating their core performances (biological characters) and their fitness values. The fitness of an individual, similar to the adaptability of an organism to the environment, is a representation of how well the core performance fits to the pre-defined optimization objectives. Individuals with higher levels of fitness functions are believed to be stronger ones and thus reproduced into next generation. These selected individuals are regarded as parents and their core designs are extracted out to formulate a mating pool for reproduction purpose. Crossover is performed to mix core designs from different parents. Design variables of parental individuals are split and merged randomly to produce offspring individuals. In order to prevent stagnation and increase diversity of the population, a mutation operation is performed to randomly alter one or more design variables such that the offspring individuals may have very different design variables as those of the parental individuals.

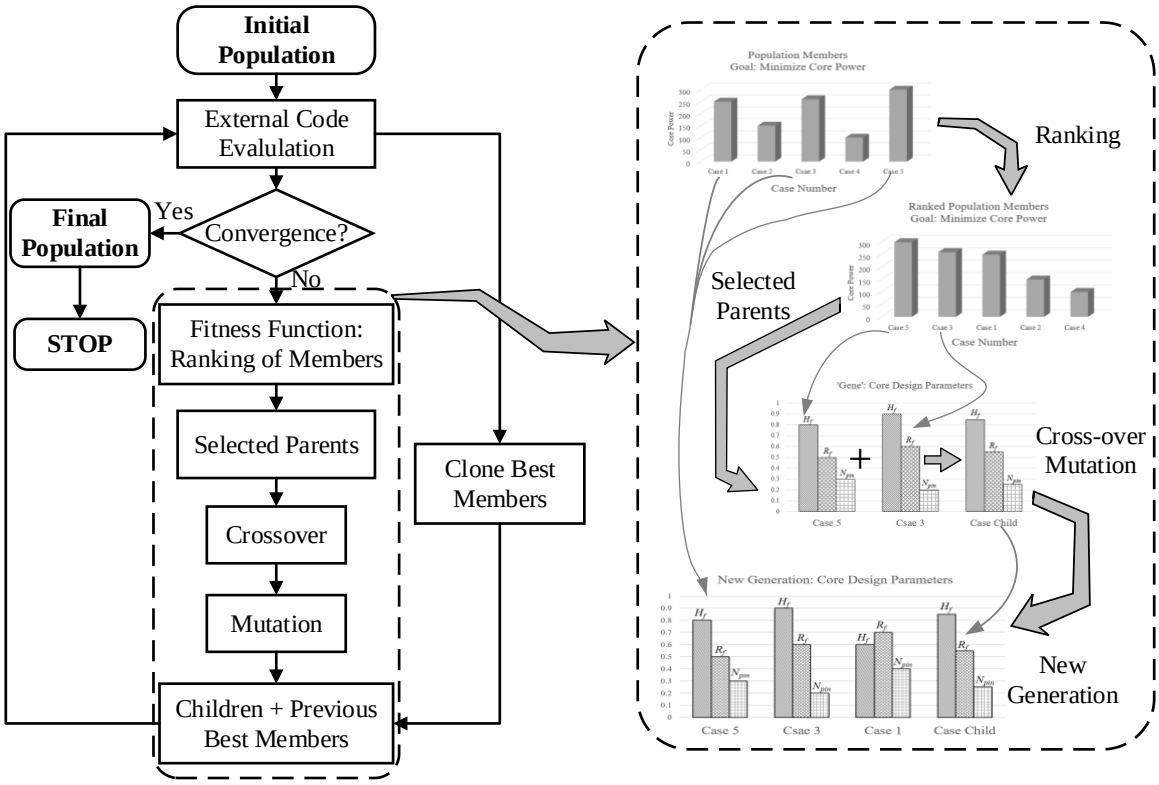

Fig. 5 – Genetic algorithm based optimization method.

Fig. 6 further illustrates the determination of fitness values for different individuals. All of the members in the current generation are ordered by counting the number of solutions by which it is dominated. The non-dominated solutions, generally located in the Pareto Front, are assigned to ranking value of 0. The dominated solutions are assigned to different rankings depending on the number of solutions that dominate them. The fitness of an individual is then assigned as the negative value of the number of dominators. The selection process of the solutions with largest fitness values is performed by passing individuals with fitness values larger than -10 into the next generation. This selection process realizes the principles of ‘the fitter individuals will survive’ and ‘newer generation fits better to environment’, while the operations of cross over and mutation ensure the

global exploration of the input space. Therefore, core designs at the final generation are regarded as global optima when optimization convergence is achieved.

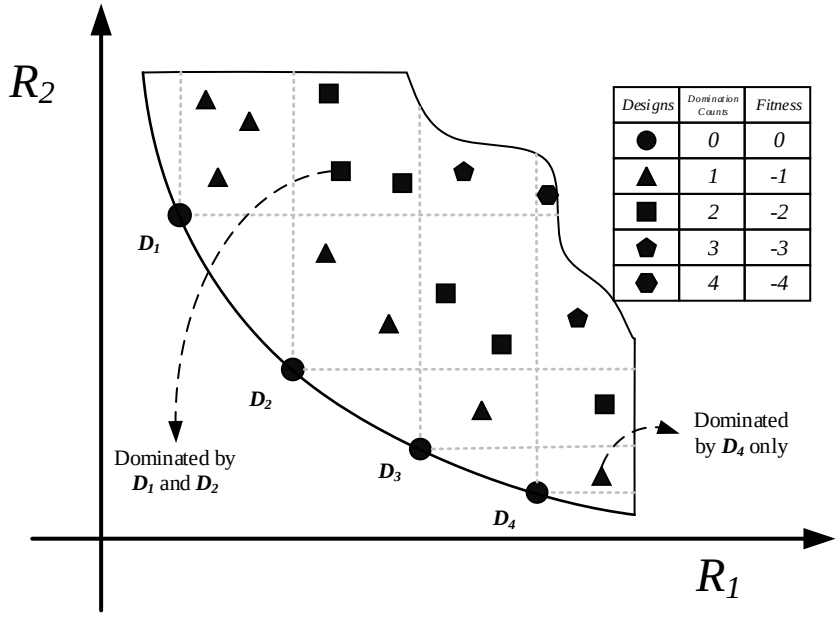

Fig. 6 – Ranking individuals: the number of dominating solutions.

3.6 Step 4: Refining the Setup of Optimization Problem

The ABTR core optimization with multi-objective genetic algorithm (MOGA) and direct physics simulation is performed in this study, and simulation results will be presented in Section 4. Although the MOGA method is capable of effectively exploring the input space and producing global optimal solutions, usually it requires a large number of individual evaluations at the order of ten thousand before achieving convergence. Given that each evaluation of core design using direct physics simulation takes ~ 13 minutes, it is important to refine the setup of the optimization problem to reduce computational time.

A surrogate model is built to ease the computational burden using the Gaussian Process technique. Gaussian Process (GP), also known as Kriging, is a kind of machine

learning technique that builds fitting functions from given training data, which is generated from the original physics model using ARC code. The goal of the surrogate model is to reproduce outputs accurate enough over the whole input design space. DAKOTA is capable of building surrogate model from training data sets and predict outputs at unknown data points. A general GP fitting function can be represented with Eq. (1) [19]:

$$\hat{f}(\underline{x}) \approx \underline{g}(\underline{x})^T \underline{\beta} + \underline{r}(\underline{x})^T \underline{\underline{R}}^{-1} (\underline{f} - \underline{\underline{G}}\underline{\beta}) \tag{1}$$

where $\underline{x}$ is the input data points, $\underline{g}(\underline{x})^T \underline{\beta}$ together represents the trend function, with $\underline{g}(\underline{x})$ being the trend basis function and the coefficients $\underline{\beta}$ determined from the least-square fit of the training data set. $\underline{r}(\underline{x})$ is the correlation vector between the current data point $\underline{x}$ and the rest data points. $\underline{\underline{R}}$ and $\underline{\underline{G}}$ are matrixes evaluated by taking all the data into account and represent the correlation and the value of trend basis function, respectively. Finally, $\underline{f}$ represents the responses and $\hat{f}(\underline{x})$ is the prediction at the current data point.

There are multiple methods that can be applied to calculate the accuracy of the surrogate model. In this study, the relative mean squared error (*RMSE*, Eq. (2)) and absolute mean square error (*MSE*, Eq. (3)) are adopted for global quality assessments.

$$RMSE = \sqrt{\frac{1}{N}\sum_{i=1}^{N}\left(\frac{\hat{R}_{SR,i} - R_{phys,\,i}}{R_{phys,\,i}}\right)^2} \tag{2}$$

$$MSE = \sqrt{\frac{1}{N}\sum_{i=1}^{N}\left(\hat{R}_{SR,i} - R_{phys,\,i}\right)^2} \tag{3}$$

where, N is the number of data points for quality assessment. $\hat{R}_{SR,i}$ and $R_{phys,\,i}$ stands for the prediction of the surrogate model and output from physical ARC calculation at the input

core design data point of $\underline{x_i}$, respectively. $\overline{R_{phys,\,i}}$ is the average value of all the $R_{phys,\,i}$. The results of this analysis applied to ABTR optimization are presented in Section 5.

3.7 Step 5: Selection of Final Candidate Core Designs

Core designs located in Pareto Frontier are optimal solutions suggested by the multi-objective optimization method, each of which reflects the trade-off among different core performance. It depends on the users' consideration to select the final optimal core designs from the Pareto Frontier, while multiple methods could be applied to aid this decision-making process.

An example of decision-making process is introduced in this paper by simply calculating the normalized weighted distance from data points in Pareto Frontier to the so-called ideal core performance, which is artificially constructed with the best core response values available in the Pareto Frontier. As shown in Fig. 7, the user-specified constraints are applied to the solution space and the Pareto Frontier is obtained with the solutions from the final population. Data point P_1 contains the best value of core response variable R_1, denoted as R_{1best}, while the best value of R_2 is observed at point P_2 and denoted as R_{2best}. The ideal core performance is determined as (R_{1best}, R_{2best}), which is constructed by taking the best values of those two objectives. According to the problem setup, the Pareto Frontier of ABTR optimal core design is a 5-dimensional space, while the ideal core performance is consisted by the minima of reactivity swing, Pu mass feed, core power and core volume, as well as the maxima of peak fast flux available in the Pareto Frontier.

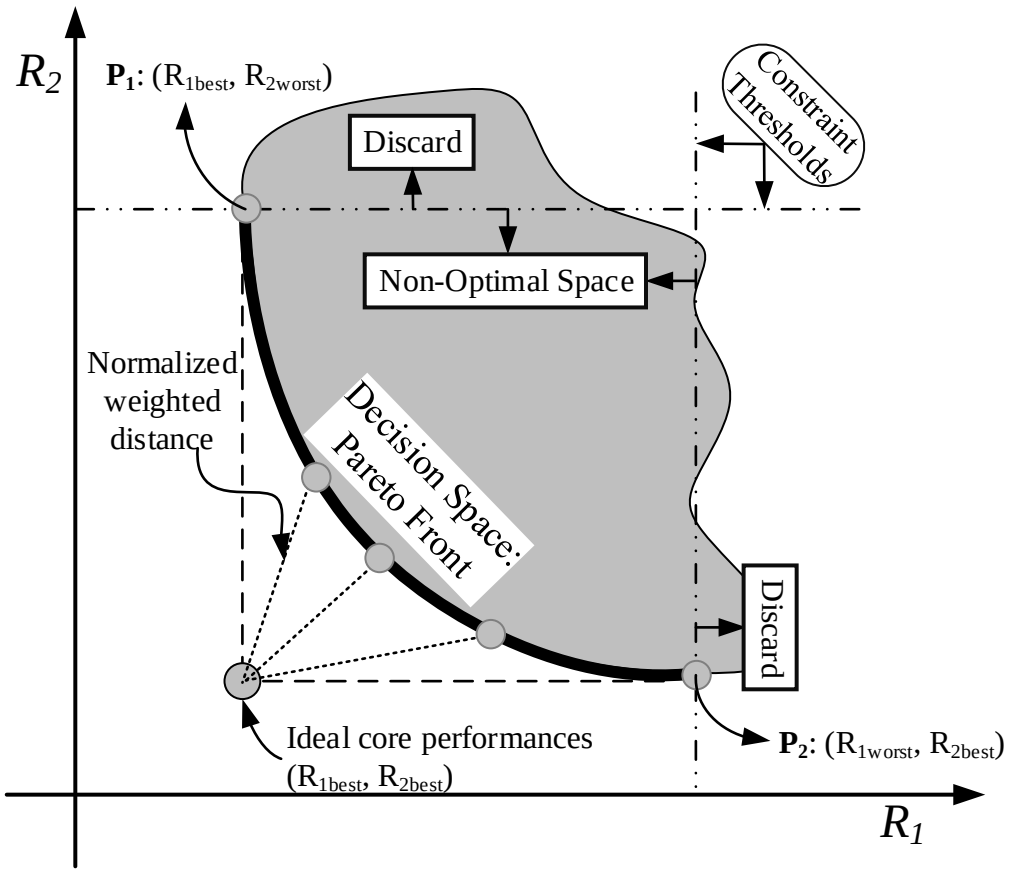

Fig. 7 – Selection of final candidate core designs from Pareto Frontier.

By assigning different weights to core performance responses as shown in Table V, the candidate core designs can be selected out as the one with minimum normalized weight distance to the data point of ideal core performance. The normalized weighted distance is calculated with the following Eq. (4):

$$D_i = \sqrt{\sum_{j=1}^{5} w_j \times \left(\frac{R_{i,j} - R_{i,j}\big|_{best}}{R_{i,j}\big|_{worst} - R_{i,j}\big|_{best}} \right)^2} \tag{4}$$

where D_i is the weighted distance corresponding to core design data point of $\underline{x_i}$, $R_{i,j}$ representes the value of the j_{th} core objective response of different data points, $R_{i,j}\big|_{best}$ is

the best core performances, $R_{i,j}\big|_{worst}$ is the worst core performances, and w_j is the weights assigned to $R_{i,j}$. The distance estimation of $\left(R_{i,j}\big|_{worst} - R_{i,j}\big|_{best}\right)$ serves as a scaling factor for normalization purpose.

Table V – Weights w_j used for selecting candidate core designs.

	Reactivity swing	Pu Mass Feed	Core Power	Core Volume	Peak Fast Flux
CAND.1	100%	0%	0%	0%	0%
CAND.2	0%	100%	0%	0%	0%
CAND.3	0%	0%	100%	0%	0%
CAND.4	0%	0%	0%	100%	0%
CAND.5	0%	0%	0%	0%	100%
CAND.6	20%	20%	20%	20%	20%

4. Multi-Objective Optimization Results for ABTR

The ABTR core optimization is performed using DAKOTA based on the optimization framework illustrated in Section 3. In total, ~ 3150 optimal core designs are observed in the Pareto Frontier, and the distributions of their core performances are depicted in Fig. 8. The histograms display the frequency distributions of different core performances, which also reflect the trends of the core performances in the Pareto Frontier. The pairwise scatter plots represent the bivariate correlations, which are consistent with those observed in Table IV. Relatively strong correlation coefficients are observed from reactivity swing and core volume. Moreover, strong positive coefficients are observed between peak fast flux and both reactivity swing and core power, meaning that unfortunately maximizing peak fast flux are strongly antagonistic to the minimization of those two performances.

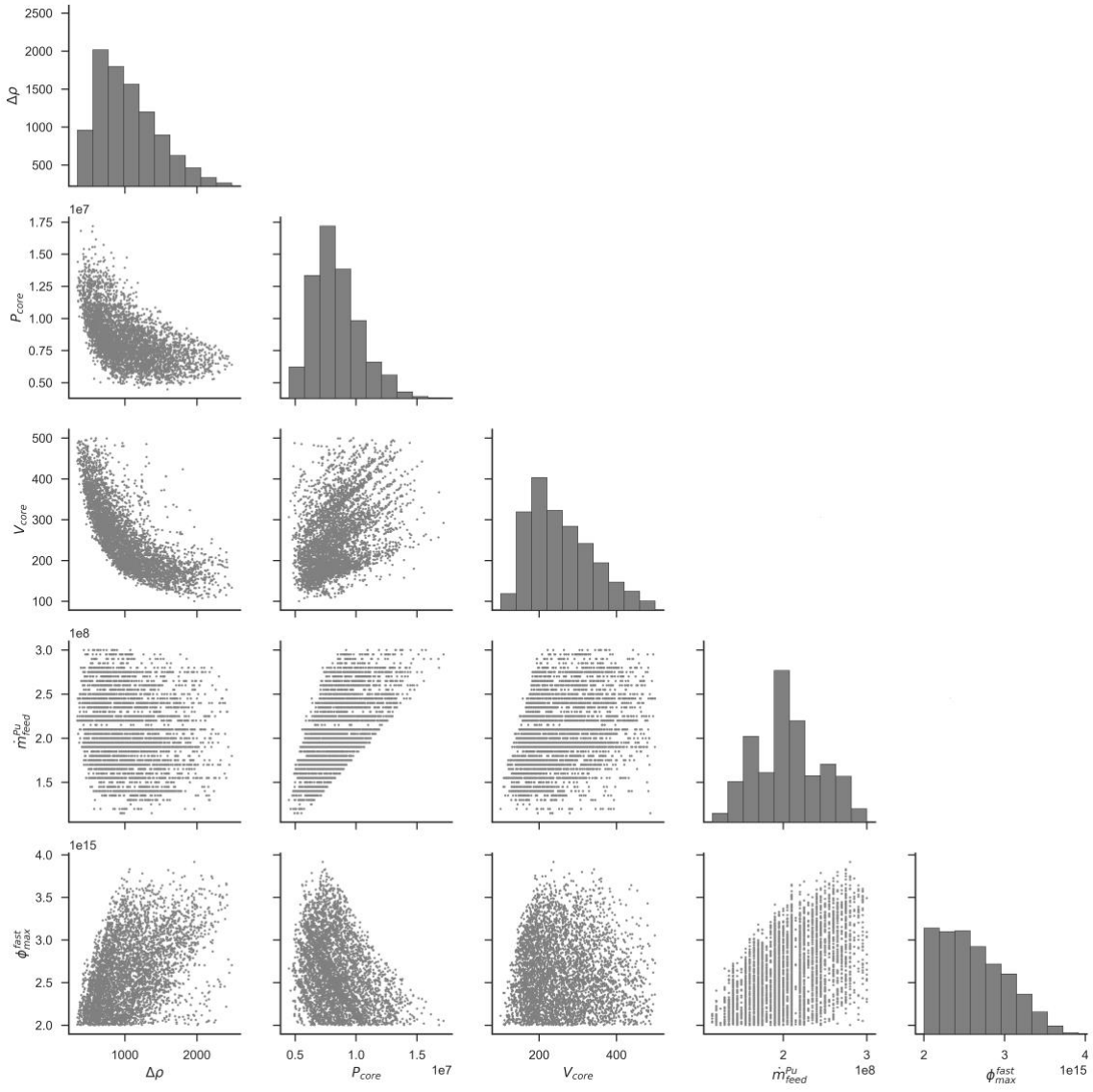

Fig. 8 – Optimal Pareto Frontier and its 2-D projections.

Six optimal core design candidates are selected based on the weights presented in Table V. Refined neutronic simulations of those candidate core designs are performed with the VARIANT nodal transport solver. As shown in Table VI, all of the six candidates show better compromises of core objective performances compared with the reference core configuration. CAND. 1 represents the configuration with the smallest reactivity swing

available in the Pareto Frontier, while CAND. 2 – 5 represent the core design with best performances in core power, volume, Pu mass feed, and peak fast flux, respectively. CAND. 1 has slightly smaller reactivity swing and Pu mass feed compared to the reference core configuration, while the core power and volume is significantly reduced and peak fast flux is increased. The additional CAND. 6 is selected out as a balance of core performance by assigning same weight to all of the five objectives. The CAND. 3 and CAND. 6 are obtained to be the same, which implies that the impact of core volume is more significant compared to the rest of the four objectives. Fig. 9 shows the core performances of the six candidates, while the value of different core responses are normalized to the value obtained from the reference core configuration. It should be noted that an upper bound of 2500 pcm is enforced in the reactivity swing during optimization, and thus CAND. 2 – CAND. 6 show larger reactivity swing compared to reference core design, which reflects compromise among five core performances, and does not mean that those candidate designs are not optimal designs.

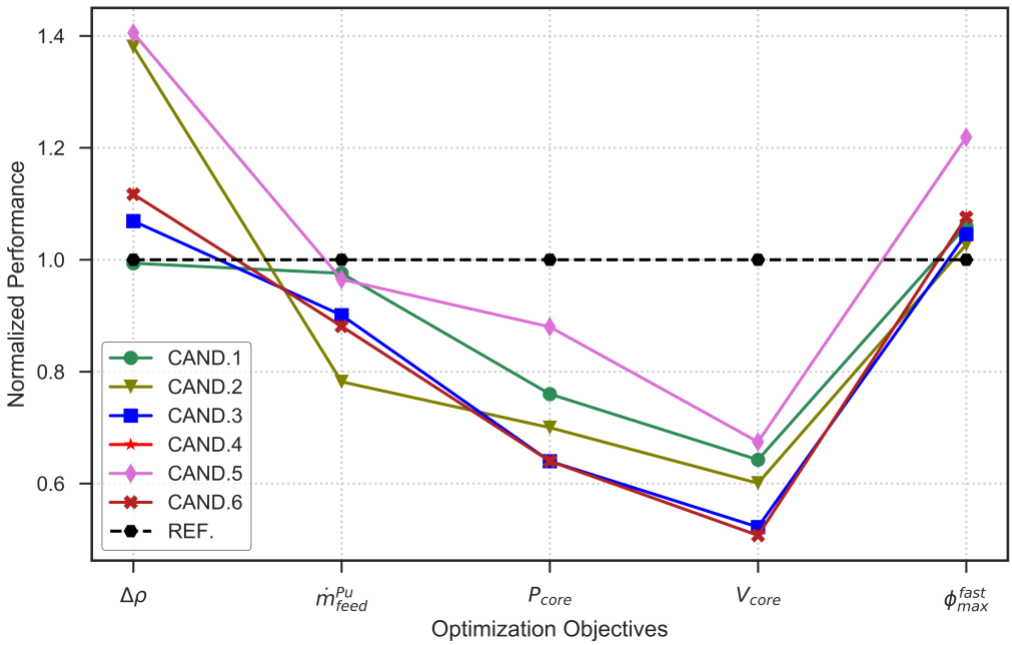

Fig. 9 – Core performances of different candidate designs.

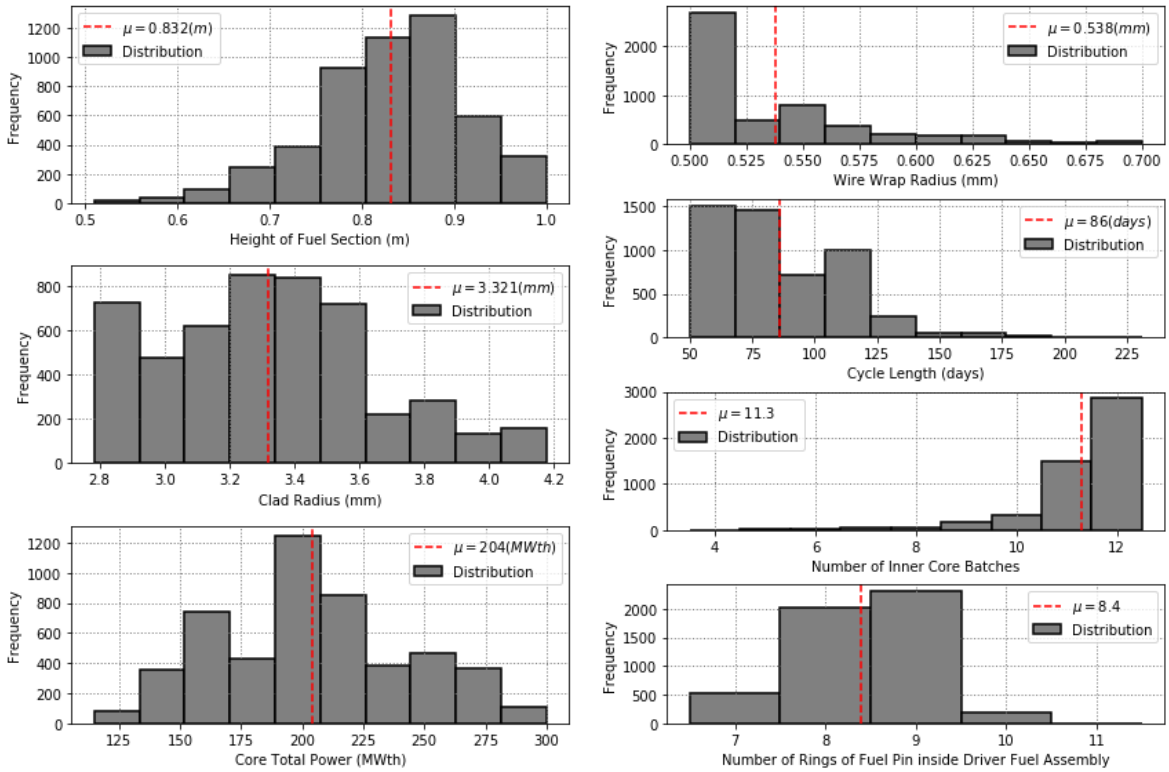

Fig. 10 – Distribution of core design parameters in Pareto Frontier.

The distribution of optimal core design parameters located in the Pareto Frontier is presented in Fig. 10. It is found that the optimal design parameters are mostly distributed in the central region of the predefined range for parameters including the height of the fuel region, clad radius, core power and number of pin rings of fuel assembly. However, the optimal wire-wrap radius and number of inner core batches tend to locate in the left and right boundaries of the predefined ranges, respectively. It should be noted that extending the exploration ranges of these input parameters during optimization would include more possibilities. However, the design range is also limited due to manufacturing and fuel management considerations and is not expanded in this study.

Table VI – Optimal core performance obtained with different weights.

Output Quantities of Interests	Ref. *	CAND. 1	CAND. 2	CAND. 3	CAND. 4	CAND. 5	CAND. 6
Δρ (pcm)	1415	1406(0.6%)	1513	1581	1954	1988	1581
Core power (MW)	250	190	160(36%)	160	175	220	160(36%)
Core volume (m^3)	9.7	6.2	5.1	4.9(47%)	5.8	6.5	4.9(47%)
Pu mass feed (kg/year)	178	174	160	157	139(22%)	172	157(12%)
Peak fast flux (10^{15} n/cm^2-s)	2.8	3.0	2.9	3.0	2.9	3.4(21%)	3.0(7.1%)
Plutonium weight fraction required (w.t.%)	0.21	0.26	0.29	0.3	0.28	0.3	0.3
Peak fast fluence (10^{23} n/cm^2)	3.6	2.9	2.8	2.8	3.5	3.6	2.8
Peak discharge burnup (GWd/t)	138	133	137	143	166	178	143
Pressure drop along fuel pin (MPa)	0.24	0.33	0.41	0.39	0.3	0.28	0.39
Peak cladding temperature with 3 σ HCF (^oC)	641	650	642	646	649	650	646
BOC Peak fuel temperature (^oC)	730	769	738	746	759	736	746
EOC Peak fuel temperature (^oC)	728	766	735	743	755	732	743
Sodium void worth ($)	-0.35	-1.76	-2.07	-2.48	-2.67	-2.70	-1.76
Height of the driver fuel column (cm)	80	85	81	83	79	67	85
Radius of inner cladding surface (cm)	0.348	0.347	0.338	0.308	0.308	0.282	0.347
Radius of the wire-wrap structure (cm)	0.0515	0.0573	0.0563	0.05	0.05	0.0515	0.0573
Cycle length (days)	120	95	127	90	90	100	95
Number of inner core batch	12	12	11	12	12	12	12
Number of pin rings inside fuel assembly	9	7	7	7	7	9	7

*: ABTR reference core performance and configuration.

5. Supplemental Studies

5.1 Gaussian Process based surrogate model

The computational time required for the optimization with direct physics simulation is 6,171 hours, which is computationally expensive for a predesign procedure. The direct physics simulation is replaced by evaluating the surrogate model to reduce the computational time to 617 hours. The optimal core designs located in Pareto Frontier are obtained with multi-objectives optimization. The surrogate model is built with 2000 data sets obtained from the direct physics calculation, and further verified with 1000 data sets. The *RMSE* and *MSE* of the surrogate model predictions is calculated, as shown in Fig. 11. The relative error of most output variables is well below 10%, indicating the surrogate model is capable of representing the core characteristics. Although a large *RMSE* of 37% is observed for sodium void worth, it is considered acceptable because its *MSE* is only 0.06 $ and the sodium void worth is used as a design constraint with an upper bound of 2 $.

Similarly, the six candidate optimal core designs are selected out and simulated with VARIANT nodal transport solver. The simulation results compared with reference core configuration are depicted in Fig. 12. Note that CAND. 4 overlaps with CAND. 6. Comparing CAND. 2 with CAND. 5, it clearly shows that to improve the performance of Pu mass feed and core power, the performances in peak fast flux and reactivity swing deteriorate significantly.

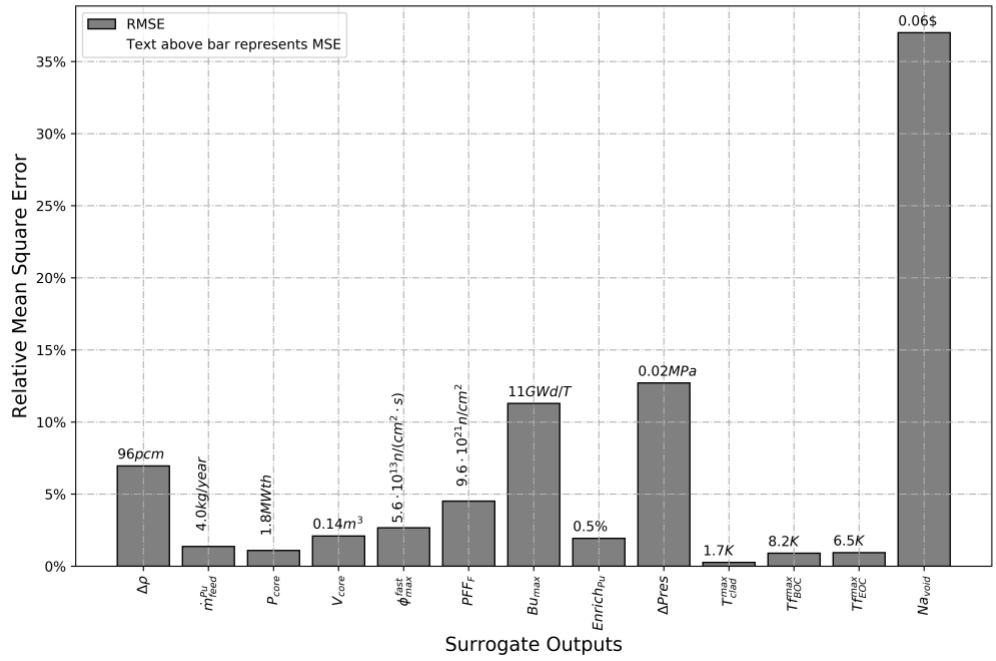

Fig. 11 – Verification of surrogate model.

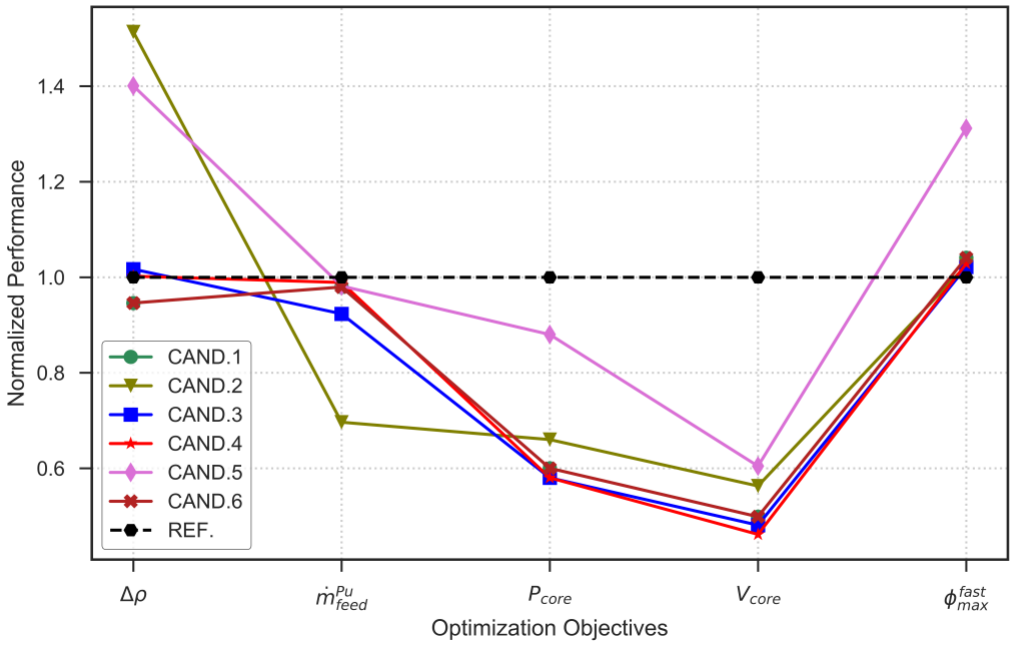

Fig. 12 – Candidate core designs obtained with the use of surrogate model.

5.2 Impact of Selection of Design Objectives

The use of surrogate model reduces the time required for a core evaluation. Another efficient way of saving computational time is to reduce the number of objectives, which could efficiently speed up the optimization convergence. As shown in Table IV, the reactivity swing and core volume are highly correlated with other objectives, which implies that these two variables have strong linear variations with respect to other variables, and could be automatically optimized while improving the rest of three objectives.

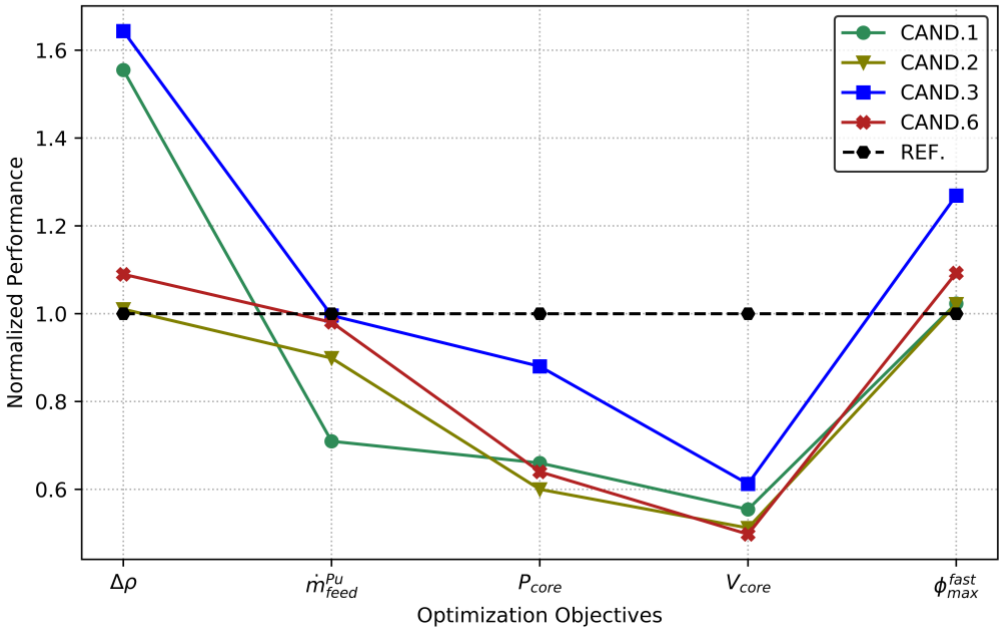

Fig. 13 – Candidate core designs obtained from optimization with reduced objectives.

A new optimization calculation has been performed with three optimization objectives: maximizing peak fast flux, minimizing core power and Pu mass feed. The number of core evaluations required for optimization convergence reduced from 31,653 to 24,562. As depicted in Fig. 13, four candidate core designs are selected out, and all of the

candidates show better core objective performances compared with reference core configuration. A minimum Pu mass feed of 126 kg/year is observed from CAND. 1, which is 52 kg/year less than reference core configuration. Comparison of CAND. 2 and CAND. 3 shows the trade-off between core power and peak fast flux: in order to improve the peak fast flux from 2.9×10 n_{15}/cm_2-s to 3.1×10 n_{15}/cm_2-s, the power needs to be increased from 150 MWth to 220 MWth.

5.3 Performance Comparison of Various Optimization Approaches

A comparison of different optimization methods is presented in Table VII, where equal weights are assigned to objectives variables to obtain core configurations with balanced core performances. It should be noted that all three core configurations reflect the trade-off among different core performances. The required computational time and sample size to reach convergence are presented in Table VIII, where the computational time is factored as the time required when each sample is executed serially.

The reactivity swing and core volume are strongly correlated with other objectives. Consequently, removing them from the list of objectives does not have large impacts on the results, but reduces the required convergence sample size by 7,091. The use of surrogate models reduces the computational time by 5,554 hours and 6,965 hours, respectively, compared with approaches when using physics-based calculation to optimize 3 and 5 objectives. Generating the data for surrogate model buildup consumes 586 hours, but the optimization process is relatively fast and only takes 31 hours. Therefore, the surrogate-based multi-objective optimization is considered as the best approach due to the significant saving in computational time and satisfactory accuracy.

Compared with the human-driven optimization process, which is usually an iterative procedure among different physics domains and performed by different teams, the merit of the proposed optimization framework is to save human effort, which is much more expensive than machine cost. Setting up an optimization problem does require some experience from designer in terms of reactor physics and core design. A sensitivity analysis is recommended in this framework, which reveals the physics insight and correlations among input reactor design parameters and output performance objectives. Such analyses are useful to teach the designer the impact of some design parameters on different core output results. Another advantage of the proposed framework compared to the human-driven optimization process is that it is capable of providing several optimized core designs options satisfying several optimization objectives. Finally, the optimization setup can be easily re-run with more or less input parameters, degrees of freedom, technological solutions in a straightforward way to a user.

Table VII – Comparison of optimal configuration suggested by different methods.

Output Quantities of Interests	**Ref.** *	**MOGA with 3 objectives**	**Surrogate based optimization with 5 objectives**	**MOGA with 5 objectives**
Δρ (pcm)	1415	1542	1338	1581
Core power (MW)	250	160	150	160
Core volume (m^3)	9.7	4.8	4.8	4.9
Pu mass feed (kg/year)	178	175	174	157
Peak fast flux (10^{15} n/cm^2-s)	2.8	3.1	2.9	3.0
Plutonium weight fraction required (w.t.%)	0.21	0.3	0.29	0.3
Peak fast fluence (10^{23} n/cm^2)	3.6	2.5	2.3	2.8
Peak discharge burnup (GWd/t)	138	130	123	143
Pressure drop along fuel pin (MPa)	0.24	0.42	0.31	0.39
Peak cladding temperature with 3 σ HCF (^oC)	641	646	646	646
BOC Peak fuel temperature (^oC)	730	746	746	746
EOC Peak fuel temperature (^oC)	728	743	750	743
Sodium void worth ($)	-0.35	-2.81	-3.03	-1.76
Height of the driver fuel column (cm)	80	80	74	85
Radius of inner cladding surface (cm)	0.348	0.302	0.312	0.347
Radius of the wire-wrap structure (cm)	0.0515	0.0500	0.0515	0.0573
Cycle length (days)	120	85	75	95
Number of inner core batch	12	11	12	12
Number of pin rings inside fuel assembly	9	7	7	7

*: ABTR reference core performance and configuration.

Table VIII – Comparison of computational resources required for different methods.

	MOGA with 3 objectives	Surrogate based optimization with 5 objectives	MOGA with 5 objectives
Computational time (h)	6171	586 + 31	7582
Convergence sample size	24562	35695	31653

6. Conclusions and Future Work

Due to the large number of design parameters, the nonlinearities among inputs and outputs, and complicated fast reactor fuel cycle management strategies, sodium cooled fast reactor SFR core concepts have been developed typically based on the intuition and experience of fast core designers. However, a full computational framework for optimizing SFR based on multi-objectives has been proposed, developed, and successfully applied to the Advanced Burner Test Reactor (ABTR) core design with optimization methods based on the genetic algorithm. The NEAMS Workbench, which integrates the ARC suite of codes through PyARC module and DAKOTA, are used for core modeling, sensitivity analysis, surrogate model build-up and design optimization of the ABTR core. Finally, a set of near optimal core designs located in the vicinity of the Pareto Frontier are selected, which reflects the trade-off among different core optimization objectives.

The optimization problem is set up by selecting a total number of five core performance parameters as the optimization objectives. The input space is established initially with expert opinion and further verified by the global sensitivity analysis, in which a set of important input parameters with potential significant impacts on core optimization objectives is identified. The statistical correlation is drawn from the core responses, which measures the global linearity among different variables. Large values of linear correlation coefficients are found for the reactivity swing and core volume, indicating their dependency on other parameters, while the rest three objective variables show higher degree of independence. The optimization process based on the genetic algorithm results in a group of near-optimal core designs and the selection of final candidate designs near the Pareto Frontier is a decision-making process, where different solutions could be picked depending

on the specific considerations of the designer. This study shows an example of selecting candidate core designs using the normalized distance to the ideal data point.

Two additional studies are conducted to accelerate the optimization process: in the first approach, the physics model is replaced by the fast running surrogate model based on the Gaussian Process; in the second approach, the number of optimization objectives is reduced based on the sensitivity analysis results. The results comparison suggests that the surrogate based multi-objective optimization is preferred due to its capability of saving computational time and resources, while maintaining relatively high predictive accuracy. It is worth mentioning that a large discrepancy is found in the sodium void worth prediction using the surrogate model; however, this is acceptable because sodium void worth is only used as an optimization constraint, and an accurate transport simulation is performed for the final core design as the final stage of the optimization.

The SFR optimization framework shown in this work has been developed in a code-agnostic way such that the simulation model (i.e., ARC) can be seamlessly replaced by any other reliable neutronics models. This feature helps facilitate the transition to high-fidelity codes or even the multi-physics simulation capability, which couples the neutronics, thermal-hydraulics, fuel performance codes, under both steady-state and transient conditions.

In the future, this optimization study will be transposed to optimization of the Holos-Quad reactor [30], with a larger degree of freedom in the input space and an extended list of multi-physics optimization objectives. It attracts the authors' attention that building the surrogate model for sodium void worth is challenging, and more data should be generated for building a more accurate model with a deep machine learning technique,

such as artificial neutral network. Multi-objective genetic algorithm is selected as the optimization kernel in this study, which is capable of searching for global optima but with relatively large sample size for optimization convergence. It is worthwhile to investigate other optimization methods with improved computational efficiency. One popular approach would be the use of hybrid method, which has been implemented in the DAKOTA code and employs a global optimization algorithm for the first several generations to narrow down the region of interest, and then switches to local optimization method for a fast convergence by searching the vicinity of the identified region.

Acknowledgements

The authors would like to express their sincere appreciation to Dr. Laura Swiler of Sandia National Laboratory (SNL), Robert A. Lefebvre of Oak Ridge National Laboratory (ORNL), and Dr. Kostadin Ivanov of North Carolina State University (NC State) for their technical assistance, discussion, and suggestions. This paper was created with the support from the Energy's Nuclear Energy Advanced Modelling and Simulation (NEAMS) Campaign.

References

[1] D. Rozon and M. Beaudet, "Canada Deuterium Uranium Reactor Design Optimization Using Three-Dimensional Generalized Perturbation Theory," *Nuclear Science and Engineering*, pp. 1-20, October 1991.

[2] C. Darwin, The Origin of Species by Means of Natural Selection, London: Routledge, 1859.

[3] J. Holland, Adaptation in Natural and Artificial Systems, Ann Arbor: University of Michigan, 1975.

[4] C. Pereira and C. Lapa, "Coarse-Grained Parallel Genetic Algorithm Applied to a Nuclear Reactor Core Design Optimization Problem," *Annals of Nuclear Energy*, pp. 555-565, September 2002.

[5] H. Sayyaadi, and T. Sabzaligol, "Various Approaches in Optimization of a Typical Pressurized Water Reactor Power Plant," *Applied Energy*, p. 1301–1310, 2009.

[6] R. Omori, et al., "Applications of Genetic Algorithms to Optimization Problems in the Solvent Extraction Process for Spent Nuclear Fuel," *Nuclear Technology*, pp. 26-31, 2 October 1996.

[7] F. Alim, et al., "New Genetic Algorithms (GA) to Optimize PWR Reactors Part I: Loading Pattern and Burnable Poison Placement Optimization Techniques for PWRs," *Annals of Nuclear Energy*, pp. 93-112, 2008.

[8] F. Alim, et al., "New Genetic Algorithms (GA) to Optimize PWR Reactors Part II: Simultaneous Optimization of Loading Pattern and Burnable Poison Placement for the TMI-1 Reactor," *Annals of Nuclear Energy*, pp. 113-120, 2008.

[9] F. Alim, et al., “New Genetic Algorithms (GA) to optimize PWR Reactors Part III: The Haling Power Depletion Method for In-core Fuel Management Analysis,” *Annals of Nuclear Energy*, pp. 121-131, 2008.

[10] E. Hourcade, et al., “SFR Core Design : A System-Driven Multi-Criteria Core Optimisation Exercise with TRIAD,” in *Fast Reactor Conference FR13*, 2013.

[11] X. Ingremeau, et al., “FARM: A new tool for optimizing the core performance and safety characteristics of Gas Cooled Fast Reactor cores,” in *International Congress on Advances in Nuclear Power Plants*, Nice, France, 2011.

[12] E. Hourcade, et al., “Innovative Methodologies for Fast Reactor Core Design and Optimization,” in *International Congress on Advances in Nuclear Power Plants*, Nice, France, 2011.

[13] A. Kumar, et al., “A New Approach to Nuclear Reactor Design Optimization Using Genetic Algorithms and Regression Analysis,” *Annals of Nuclear Energy*, pp. 27-35, May 2015.

[14] O. Fabbris, et al., "Surrogates Based Multi-Criteria Predesign Methodology of Sodium-Cooled Fast Reactor Cores – Application to CFV-like Cores," *Nuclear Engineering and Design*, pp. 314-333, 2016.

[15] B. Rearden, “Introduction to the Nuclear Energy Advanced Modeling and Simulation Workbench,” in *International Conference on Mathematics & Computational Methods Applied to Nuclear Science & Engineering*, Jeju, Korea, 2017.

[16] B. Rearden, et, al., “NEAMS Worbench 1.0 Beta,” Oak Ridge National Laboratory, Oak Ridge, TN, U.S.A., 2018.

[17] R. Lefebvre, et, al., "NEAMS Workbench 1.0 Beta Status," in *ANS Annual Meeting*, Philadelphia, Pennsylvania, U.S.A., 2018.

[18] N. Stauff, et al., "Argonne Reactor Computation Codes Integration in the NEAMS Workbench," in *ANS Summer Meeting*, Philadelphia, PA, U.S.A., 2018.

[19] B. Adams, et al., "Dakota, A Multilevel Parallel Object-Oriented Framework for Design Optimization, Parameter Estimation, Uncertainty Quantification, and Sensitivity Analysis: Version 6.5 User's Manual," Sandia National Laboratory, Albuquerque, NM, U.S.A., 2016.

[20] L. Swiler, et al., "Integration of Dakota into the NEAMS Workbench," Sandia National Laboratories, U.S.A., 2017.

[21] N. Stauff, et al., "Application of the Interface Between Dakota and the Argonne Reactor Computation Codes in the NEAMS Workbench," in *Transactions of the American Nuclear Society*, Philadelphia, PA, U.S.A., 2018.

[22] Y. Chang, et al., "Advanced Burner Test Reactor Preconceptual Design Report," Argonne National Laboratory, Lemont, IL, U.S.A., 2006.

[23] C. Lee and W. Yang, "MC2-3: Multigroup Cross Section Generation Code for Fast Reactor Analysis," ANL/NE-11-41 Rev. 2, Argonne National Laboratory, Lemont, IL, U.S.A., 2013.

[24] M. Chadwick, et al., "ENDF/B-VII.0: Next Generation Evaluated Nuclear Data Library for Nuclear Science and Technology," *Nuclear Data Sheets*, vol. 107, p. 2931–3060, 2006.

[25] K. Derstine, "DIF3D: A Code to Solve One-, Two-, and Three-Dimensional Finite Difference Diffusion Theory Problems," ANL-82-64, Argonne National Laboratory, Chicago, IL, U.S.A., 1984.

[26] M. Smith, et al., "DIF3D-VARIANT 11.0: A Decade of Updates," ANL/NE-14/1, Argonne National Laboratory, Lemont, IL, U.S.A., 2014.

[27] M. Smith, et al., "VARI3D & PERSENT: Perturbation and Sensitivity Analysis," ANL/NE-13/8, Argonne National Laboratory, Lemont, IL, U.S.A., 2013.

[28] A. Waltar, et al., Fast Spectrum Reactors, New York: Springer, 2012.

[29] B. Toppel, "A User's Guide to the REBUS-3 Fuel Cycle Analysis Capability," ANL-83-2, Argonne National Laboratory, Lemont, IL, U.S.A., 1983.

[30] K. S. Allen, et al., "Feasibility Study of a Micro Modular Reactor for Military Ground Applications," *Journal of Defense Management,* vol. 8, no. 1, 2018.